Lab on a Chip

Accepted Manuscript

ROYAL SOCIETY OF CHEMISTRY

www.rsc.org/loc

Lab on a Chip

ARTICLE

Micro-/Nano-scale Electroporation

Lingqian Chang[a†], Lei Li[b†], Junfeng Shi[c†], Yan Sheng[d], Wu Lu[e], Daniel Gallego-Perez[a,f*], Ly James Lee[a,c,d*]

Received 00th January 20xx,
Accepted 00th January 20xx

DOI: 10.1039/x0xx00000x

www.rsc.org/

Electroporation has been one of the most popular non-viral technologies for cell transfection. However, conventional bulk electroporation (BEP) shows significant limitations in efficiency, cell viability and transfection uniformity. Recent advances on microscale-electroporation (MEP) resulted in improved cell viability. Further miniaturization of the electroporation system (*i.e.,* nanoscale) has brought up many unique advantages, including neglegible cell damage and dosage control capabiltiies with single-cell resolution, which has enabled the more trasnlational applications. In this review, we give insight into the fundamental and technical aspects of micro- and nanoscale/nanochannel electroporation (NEP), and go over several examples of MEP/NEP-based cutting-edge research, including gene editing, adoptive immunotherapy, and cellular reprogramming. The challenges and opportunities of advanced electroporation technologies are also discussed.

1. Introduction

Electroporation is one of the most commonly used methods for non-viral gene delivery. It has played a particularly important role in recent breakthroughs in life sciences, such as gene editing (e.g. CRISPR-Cas9)[1-3], adoptive immunotherapy (e.g. chimeric antigen receptors (CARs))[4], and cell reprogramming (induced neurons (iNs))[5, 6]. Non-viral approaches are typically classified into two categories, chemical and physical methods. Chemical methods include nanocarriers (e.g. lipoplex, polyplex), where cargo is intracellularly delivered through endocytosis followed by endosomal escape. These methods, however, tend to be slow and relatively inefficient[7]. Physical methods (*e.g.,* electroporation), on the other hand, are more straightforward and simpler to implement, as the cells can be directly permeabilized with a specific stimuli (*e.g.,* mechanical, electrical, optical, etc.), which facilitates entry of "naked" cargo (*e.g.,* DNA, RNA, proteins, etc.) into the cells[8].

Bulk electroporation (BEP) is a commercially-available and affordable technology with a relatively simple setup, where the cells and cargo are first loaded into a dielectric chamber upon which a bias (typically >1000 volts) is applied, thus causing membrane poration and diffusion/endocytosis-based cytosolic cargo delivery. Nevertheless, despite its simplicity, BEP-mediated transfection causes multiple adverse side effects, including pH changes and significant joule heating, which markedly hampers cell viability, especially in primary cell cultures[9].

Microscale electroporation (MEP) systems, which were introduced in the early 2000s[10], use a microelectrode setup that allows for the implementation of stronger and more uniform porating electric fields at significantly lower voltages compared to BEP, thus minimizing cell death. Nevertheless, like in BEP, cytosolic cargo delivery is regulated by diffusion and endocytosis-like processes, whose efficiency is considerably limited by the cargo size.

In contrast, nanoscale- or nanochannel-based electroporation (NEP) is a novel single-cell resolution transfection approach in which strong but nanoscale focused electric fields result in transfection efficiencies and cell viabilities of nearly 100%. Moreover, unlike BEP or MEP, cytosolic cargo delivery is modulated by electrophoresis, thus enabling dosage control capabilities not seen with any currently available transfection technology[11].

A number of reviews have addressed BEP or MEP-based transfection systems[9, 10, 12, 13]. Recently, we briefly touched upon a few emerging nanotechnologies for electroporation applications[14]. Here we will focus, among other things, on the research and design (R&D) efforts conducted to transition from BEP/MEP to NEP. We first describe the fundamental aspects and practical issues of BEP that led to the development of the MEP technology. Two major prototypes of MEP, including micro-electrode and microfluidic-based electroporation are briefly discussed. Finally, the recent applications of MEP and in particular NEP in cell transfection are summarized. The scenarios of using advanced electroporation devices for non-viral adoptive

[a] *Department of Biomedical Engineering, The Ohio State University, Columbus, OH, 43210, USA.*
[b] *School of Mechanical and Materials Engineering, Washington State University, Pullman, WA, 99164, USA*
[c] *Department of Mechanical and Aerospace Engineering, The Ohio State University, Columbus, OH, 43210, USA*
[d] *William G. Lowrie Department of Chemical and Biomolecular Engineering, The Ohio State University, Columbus, OH 43209 USA*
[e] *Department of Electrical and Computer Engineering, The Ohio State University, Columbus, OH 43209, USA*
[f] *Department of Surgery, The Ohio State University, Columbus, OH 43210, USA*
* E-mail: lee.31@osu.edu, gallegoperez.1@osu.edu
† These authors contribute equally.

immunotherapy, gene editing, regenerative medicine and intracellular gene interrogation will be especially highlighted.

2. Miniaturization of Electroporation

2.1 Conventional electroporation

Electroporation-based gene delivery was first reported back in 1982[15], and since then numerous studies have used this approach to introduce exogenous cargo into cells both *in vitro* and *in vivo*. Most electroporation experiments are conducted in a millimeter- to centimeter-sized chambers[16]. Fig. 1 shows a typical setup of a BEP system. A high voltage is applied across parallelly- or coaxially-arrayed electrodes immersed into the chamber, within the mixture of cells and exogenous cargo. This results in the formation of a transmembrane potential (Δ_m) across the lipid bilayer. Once Δ_m reaches a critical value, the lipid molecules within the membrane re-arrange to form small openings on the cell membrane, that facilitate cargo translocation into the intracellular space through diffusion/endocytosis[17]. A major advantage of the BEP approach is its ability to handle millions of cells. BEP-based systems have been extensively discussed in the literature[17-26]. Here we will discuss some fundamental aspects and considerations of the BEP process.

2.2 Mechanism and models of BEP

Although multiple studies have looked into the process of membrane electroporation ever since the first study on electropermeabilization was published in 1958[27], the underlying modulating mechanisms have not been fully elucidated yet, in part because of the lack of tools with high enough resolution to document the process in real time[18, 23]. A number of theoretical models on Δ_m and the process of membrane breakdown have been postulated, however, proper experimental validation of every single detail remains challenging.

BEP can be broken down into six stages: (i) application of a pulsed high voltage (around 1 kV/cm) to the electrodes; (ii) accumulation of positive and negative charges on the cell membrane; (iii) rearrangement of the lipid molecules on cell membrane once Δ_m reaches a critical value; (iv) nanopores formation on the cell membrane (*i.e.,* aqueous pathways); (v) intracellular cargo translocation mostly by diffusion/endocytosis-based processes; and (vi) membrane repair (*i.e.,* reversible electroporation or RE). However, often times, high electric fields could cause irreversible electroporation (IRE), which is known to result in cell lysis and death[28, 29].

In BEP, size disparities between the electrodes, chamber and cells lead to non-uniformly distributed electric fields at the single cell level. Different models have thus been developed for Δ_m under low cell densities[17-19, 23-25]. An example is shown in Eq. 1:

$$\Delta_m = -f \cdot E \cdot R \cdot cos\theta \cdot \left(1 - e^{-\frac{t}{\tau}}\right) \qquad (1)$$

where *f* is the form factor related to the shape of the cell, *E* is the external electric field, *R* is the radius of the cell, θ is the polar angle between the direction of *E* and a given point on the cell membrane, *t* is the lasting time of *E*, and τ is the time constant of the cell membrane. In most cases, the transient terms in Eq. 1 can be ignored as the cell membrane charging time is significantly shorter than the pulse duration ($\tau \ll t$, the pulse duration[23]) , therefore Eq. 1 can be simplified as:

$$\Delta_m = f \cdot E \cdot R \cdot cos\theta \qquad (2)$$

Eq. 2 is referred to as the steady-state Schwan equation[18]. The form factor f is 1.5 for spherical cells, and 0.5 for elongated cells[23]. Eq. 2 is commonly used to calculate Δ_m for a limited number of cellular shapes and densities. Recently, finite element methods (FEM) were used to calculate the electric field distribution and Δ_m on single cells with irregular shapes or high cell densities[18].

As discussed previously, membrane poration occurs when Δ_m reaches a critical value (Δ_s) of approximately 0.5 - 1V[17]. Poration and diffusion/electrophoresis-based cargo translocation can be described by Eq.3[18]:

$$\frac{V}{S_p}\frac{dc}{dt} = -D\frac{zEF}{\rho T}c - D\nabla c \qquad (3)$$

Where *V* is the cell volume, S_p is the surface area of the permeabilized cell membrane, *c* is the concentration of the cargo transported across the cell membrane, and *D* is the diffusion coefficient. The first term on the right side of Eq. 3 describes electrophoretic component of the process, which is dependent on the electric charge (*z*) of the molecules and the local electric field (*E*). The second term is the diffusion component, which is driven by the concentration difference (∇c) across the cell membrane. Electrophoresis is believed to be the dominant factor while the electrical stimulation is applied. Diffusion plays a more prominent role when the external electric field is turned off. It is believed that small cargo and ions transport across cell membrane through diffusion, while large cargo (*e.g.* plasmids, proteins, etc.) mainly depend on electrophoresis.

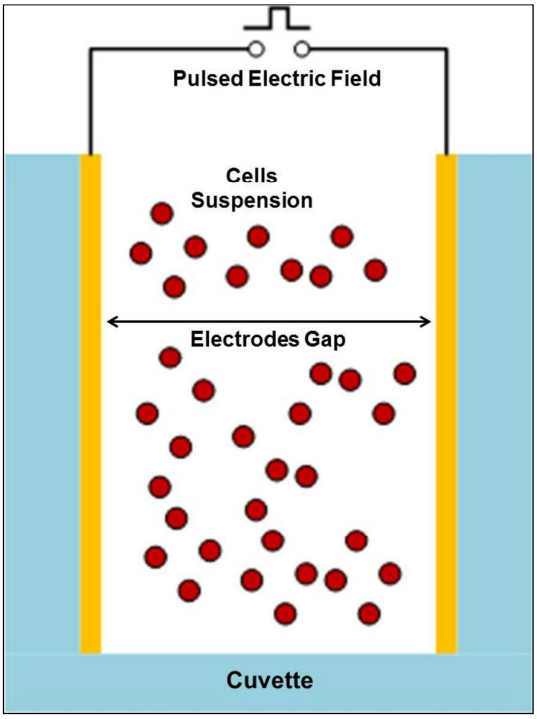

Fig.1. Schematic of a bulk electroporation system. Electrode gap is larger than the size of a single cell with several orders of magnitude.

2.3 BEP setup

Commercially available BEP systems consist of a cuvette with built-in electrodes and power supply for pulsed voltage generation (e.g. Lonza nucleofector™, Lonza Group, US). For *in vivo* applications, needle electrodes are usually used to penetrate tissues (e.g. NEPA21, NEPA gene, Japan). Various approaches have been reported to enhance the performance of BEP. Zu *et al.* added gold nanoparticles (AuNPs) in the cell buffer, and demonstrated that the transfection efficiency can be improved 2-3-fold without compromising cell viability[30]. Zhao *et al.* recently developed a flow-through BEP device[31]. Cells flow through a large tube (inner diameter, 6.8 mm) at a high rate (2×10^7 cells/min). Three groups of needle electrode arrays (0.3 mm diameter, 1 mm center to center distance) were built-in the tube. Square wave pulses were then sequentially applied on 2 of these 3 groups each time to achieve a more uniform electric field distribution. This configuration resulted in 60% transfection efficiency and 80% cell viability[31].

2.4 BEP considerations

BEP has been used to deliver a wide variety of cargo, including nucleic acids, to proteins, enzymes, and antibodies[32-34]. Recent studies, for example, have used BEP-based delivery of Cas9 protein for gene editing purposes[6, 13, 35]. Although BEP-based systems show multiple practical advantages, including (1) well-established protocols, (2) user-friendliness, and (3) high-throughput transfection, the high voltage (>1000 V) requirement continues to be a significant limitation. Eq. 2 implies an electric field as high as 1.3 KV/cm is needed in order to achieve a 1 V (Δ_m) on a spherical cell with a radius of 5 µm. If the gap between the electrodes is set to about 5 mm (typical in BEP), a bias of 650 V or higher needs to be applied to the cell/cargo mixture. Such a high voltage tends to cause a significant decrease in cell viability due to joule heating, pH changes, and bubble formation. Moreover, typical BEP experiments handle large cell numbers per transfections, which results in randomly-distributed electric fields and $\Delta_m s$ (at the single cell level). This in turn could lead to highly stochastic transfection profiles and cell lysis in most cases. Such stochasticity can be further exacerbated by the diffusion-based cargo uptake process.

3. Microscale electroporation

MEP-based systems emerged as a more benign and controllable alternative to BEP-based transfection. The first flow-through MEP device was made of a micro-machined poly(methyl methacrylate) (PMMA) chip, which consisted of a 0.2 mm × 5 mm × 25 mm channel and gold electrodes coated on both top and bottom surfaces using thermal evaporation[36]. Subsequent studies resulted in the development of many MEP-based systems[10, 16, 37-43].

3.1 MEP setup

Rubinsky and colleagues were among the first to study single-cell electroporation on a micro-hole chip[25, 44, 45], which allowed direct monitoring of the electrical current and associated membrane breakdown. Lin's group developed the first flow-through microfluidic device for cell electroporation in 2001[36]. Currently available MEP devices are mainly based on these two prototypes, namely (i) Micro-electrode electroporation (MEEP), and (ii) Flow-through microfluidic electroporation (MFEP). MEEP typically requires single-cell entrapment within a microelectrode system before the porating electric field is applied. In contrast, MFEP is based on a process where cells are continuously flowing thorough a pair of electrodes within a microfluidic channel where the porating field is applied.

MEEP can be further divided into two subgroups, i.e. localized MEEP and random MEEP. In random MEEP, tens to hundreds of cells are loaded into a micro-scale cuvette (~ 100 µm in width) and electroporated with embedded patterned microelectrodes[46, 47]. Liang's group developed a high-throughput MEP chip for siRNA delivery[46]. In this case, cells are loaded into arrays of millimeter-scale wells, which are then electroporated using patterned spiral microelectrodes (Fig. 2A, B)[46]. Numerical simulations show that an applied bias of 150 V is sufficient to generate a uniform electric field of 300 V/cm. This MEP device design was reported to achieve transfection efficiencies and cell viabilities around 90% and 80%, respectively. However, stochastic cell transfection[46] and localized cell death (Fig. 2C-E) remain challenges with this type of systems[48], [47, 49-51].

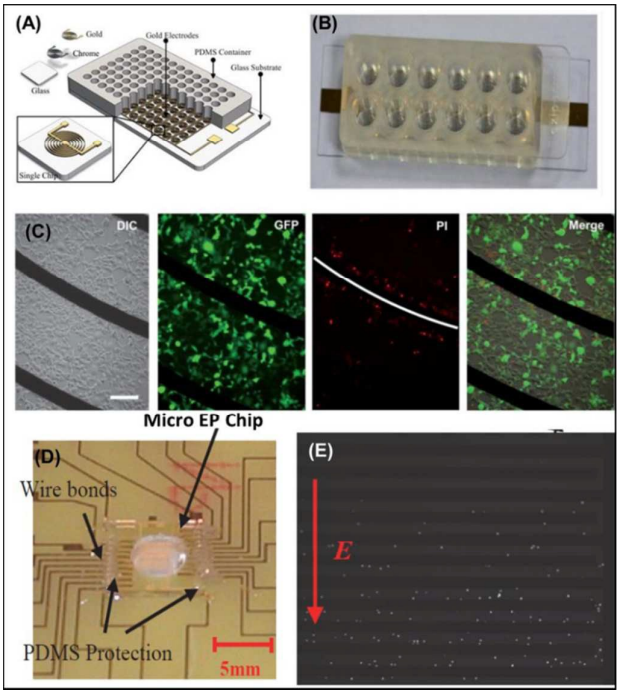

Fig. 2 Schematics and experimental setup of micro-electrode electroporation (MEEP) devices for high-throughput cell transfection. (A) Schematic diagram of the spiral-shaped micro-electrodes. (B) Assembled 12-well MEEP device. (C) Differential interference contrast (DIC) and GFP fluorescence images show the cells transfected with GFP plasmids. PI dye staining indicates dead cells after electroporation[46]. Reproduced with the permission from RSC. (D) A micro-electroporation chip that can process

thousands of cells simultaneously. (E) Fluorescence images show a gradient of transfection efficiency related to the electric field strength by using this chip[47]. Reproduced with the permission from IEEE.

Localized MEEP appears to offer additional advantages. In localized MEEPs, a micro-electrode[25, 44-46, 52-55] or micro-electrode array[56-60], with the dimensions smaller than the cell, are manufactured in the form of micro-needles and spikes, or patterned in micro-holes / nozzles / channels, etc. Highly localized electric fields are generated over a single cell or several cells so that the electric field can be intensified 2 – 3 orders of magnitude. A low-voltage (*e.g.*, <5 V) is sufficient for cell permeabilization under this configuration. The first attempts at localized MEEP focused on placing a micro-electrode, which could be carbon fiber-based[54] or an electrolyte-filled capillary [52, 55], within 10 µm of the cell to be transfected. Subsequent modifications were introduced to MEEP systems, using microfabricated systems that enabled cell alignment with the applied electric field[44] and high throughout transfection[57]. Valero *et al.* developed a device that could independently electroproate 9 cells by positioning them to 9 microholes in between two parallel channels (Fig. 3A, B)[56]. Cells are trapped towards the microholes by generating a pressure difference between two parallel channels, which essentially concentrated the electric fields at the microholes. With this configuration, biased voltage < 4 V successfully transfected the cells. Transfection efficiencies and cell viabilities hoover around 75 % and ~100 %, respectively. We developed a sandwich type MEEP for high-throughput transfection of mouse embryonic stem cells[58] (Fig. 3C).

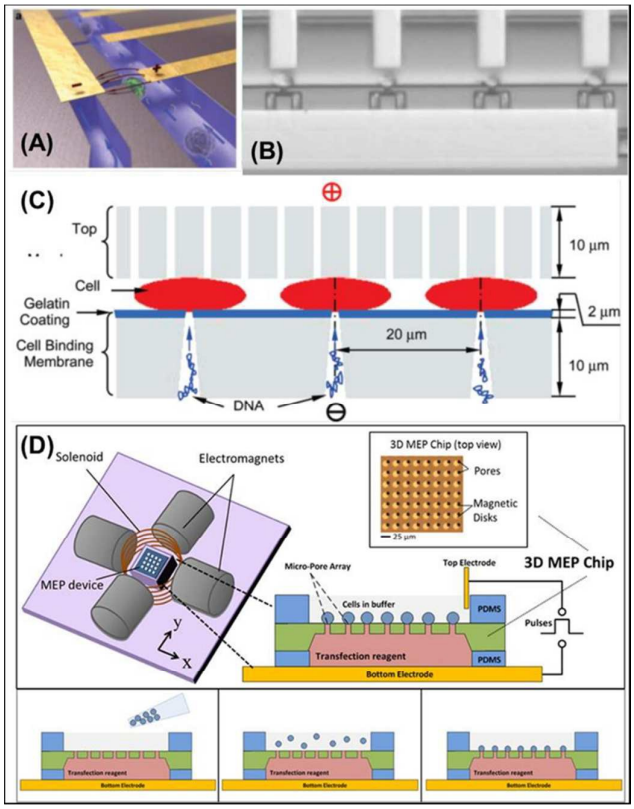

Fig. 3. Representative micro-electrode array chips for localized and high-throughput cell electroporation. (A, B) Micro-fluidic MEEP devices for single-cell electroporation[56]. Reproduced from Ref.54 with permission from RSC. (C) Micro-nozzle-based MEEP system[58]. Reproduced with permission from ACS. (D) Magnetic tweezers-based MEP platform[61]. Reproduced with the permission from Wiley.

Cells were sandwiched between two gelatin-coated polyethylene terephthalate (PET) membranes. The bottom membrane had an array of micromachined nozzles (2.5 µm in diameter), and the top membrane had track-etched pores of 1 µm. Vacuum was applied through the bottom membrane to trap each cell on a nozzles. This was then followed by the implementation of a voltage across the sandwich system to (i) localize the porating electric field on single cells, and (ii) electrophoretically drive negatively-charged cargo (*e.g.,* DNA) through each nozzle into the cytosol. Electrophoresis-driven cargo delivery in this system, however, is limited, given the fact that the applied voltage cannot exceed 20 V to avoid cell lysis[58]. In order to minimize cell damage due to vacuum forces and/or hydrodynamic cell trapping, we developed a magnetic tweezers-assisted MEEP platform[61] (Fig. 3D), where cells tethered with magnetic beads can be precisely positioned over porating silicon-based microchannels via remote control. Such system was successfully used to transfect large cell numbers (approximately 40,000 cells/cm^2) with high efficiency. Additional magnetic tweezers-based system have been reported in the literature as well[62].

MFEP-based approaches, on the other hand, transfect cells as they flow through microchannels. Porating voltages are typically applied through needle electrodes inserted into the microchannels. Recent studies, however, have used electrodes that have been directly patterned on the microchannel(s) surface. MFEP systems tend to be easier to manufacture compared to MEEP, especially considering recent advances in microfluidic technologies, and have the potential to handle a larger number of cells over the long run[36, 63-79]. Successful MFEP-based transfection requires precise synchronization between flow rate and the implementation of the porating bias. Some studies have addressed this requirement by focusing the porating electric field, often based on direct current, on a narrow portion of the microfluidic channel where only single cells can flow through[64, 67, 72, 76]. MFEP devices have been reported to handle approximately 10^4-10^8 cells per minute[73]. Different permutations of MFEP-based approaches have also been reported, including one in which single cells are transfected within oil phase droplets at relatively low voltages (4-7 V), with reported transfection efficiencies and cell viabilities of 11% and 20%, respectively (Fig. 4A)[63].

Zhu *et al.* introduced a hydrodynamic focusing electroporation device in which cells were sandwiched/transfected between two conductive fluid flows (Fig. 4B)[77]. This system reported transfection efficiencies and cell viabilities of 70% and 30%, respectively. Wei *et al.* developed a laminar flow electroporation platform that used hydrodynamic focusing to generate a buffer layer to help protect the cells from excessive electrode/solution heating, electrolysis and bubble formation (Fig. 4C)[78]. This device could achieve a 90% transfection efficiency with 60% cell viability[78]. Lu's group pioneered the development of advanced MFEP systems[80-83] for different applications, including gene delivery[84-86], intracellular molecular tracking[87, 88], and cell sampling[89, 90]. Recently, a

vortex-based MFEP system was developed to apply hydrodynamic forces and controllably rotate the cells for more uniform membrane poration (Fig. 4D)[74]. In another report, a PDMS-based MFEF system, with dimensions of 150um x 40 um x 3.8mm, was devised to investigate the dynamics of protein delivery into mouse embryonic fibroblasts[88] using a cyan/yellow fluorescent protein pair (ECFP/YPet) as model cargo. Results indicated that successful cargo translocation increased in direct proportion to the electric field, while cell viability decreased significantly at higher fields.

In addition to delivering conventional cargo such as genes and drugs, MFEF has also been used for direct delivery of proteins[40, 68, 91], which offers some advantages compared to plasmid gene delivery, including faster action, and enhanced ability to control the effective dosage.

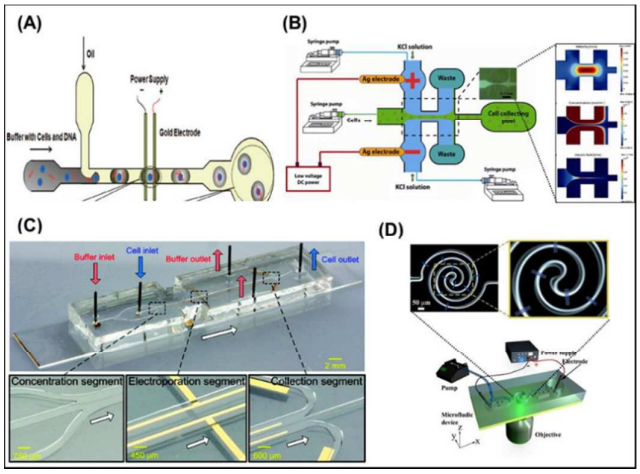

Fig. 4 MFEP-based approaches for continuous cell transfection based on a variety of designs. (A) Droplet encapsulation[63]; (B) hydrodynamic focusing[77]; (C) laminar flow electroporation [78] and (D) vortex-assisted microfluidic device[74]. Reproduced with the permissions from ACS, Springer, ACS, RSC, respectively.

In MFEP, the electrodes can be easily configured in different manners within the microfluidic device, including same patterning side[47, 63, 68, 71, 92] (Fig. 5A [68]) or opposite sides (Fig. 5B[36] and C[70]), with leads extending out of the microfluidic outlet/inlets[64, 67, 69] (Fig. 5D [67]). The electrodes at the same time can be of different shapes, such as sstripes[63], saw tooth[70], comb[68], parallel plate[36], curved stripe[46], and needle[67]. There are no restrictions on the design, dimension shapes and arrangement, and as such, the electrical field distribution and electroporation performance vary significantly from design to design.

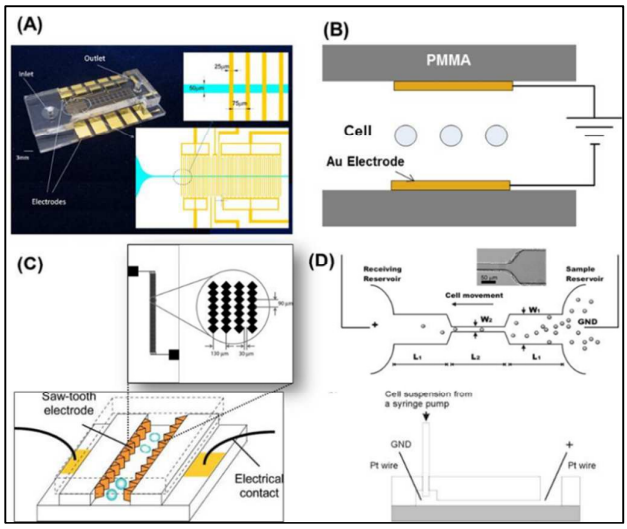

Fig. 5 MFEP devices with different designs of the electrodes, including (A) comb shaped electrodes patterned on one side of a microchannel[68], (B) parallel electrodes fabricated on both sides[36], (C) saw tooth electrodes on both sides of a microfluidic channel[70], and (D) needle type electrodes placed on the terminals[67]. Reproduced with the permissions from ACS, Elsevier, RSC and ACS, respectively.

3.2 Theoretical analysis of MEP

The major differences between MEP- and BEP-based systems stem from how the porating electric field is applied. In MEP, system miniaturization results in more localized/enhanced implementation of the electric field on individual cells, which results in successful transfection at relatively low voltages (*e.g.,* 1 V for MEP vs. >1000 V for BEP), and improved cell viability and transfection efficiencies. Moreover, MEP-based systems tend to allow concomitant *in situ* cell monitoring, and can also be interfaced with multiple systems to enable the development of advanced biointerrogation/manipulation platforms.

Multiple simulation studies have been conducted on MEP-based processes[47, 93-95]. FEM studies conducted by Movahed and Li on a particular MEP configuration (5 – 20 µm electrodes embedded within a 25 – 30 µm deep microchannel, and a 30 µm diameter cell) show that voltages between 1-3 V would result in successful membrane permeabilization around the cell poles (opposite to the embedded electrodes). Pore formation (*i.e.,* size and density) could conceivably be controlled by adjusting the electric field intensity.

Kaner *et al.* investigated how the electrode configuration influenced electric field distribution and membrane permeabilization within a microfluidic channel[94]. The results showed that the permeabilized cell hemisphere is determined by the electrode location, with a single hemisphere/pole permeabilizing when both electrodes are on the same side of the microchannel vs. both hemispheres and poles when the electrodes are on opposite sides (Fig. 6A, B)[17, 94]. The permeabilization extent was also predicted to be a function of the applied voltage (Fig. 6C).

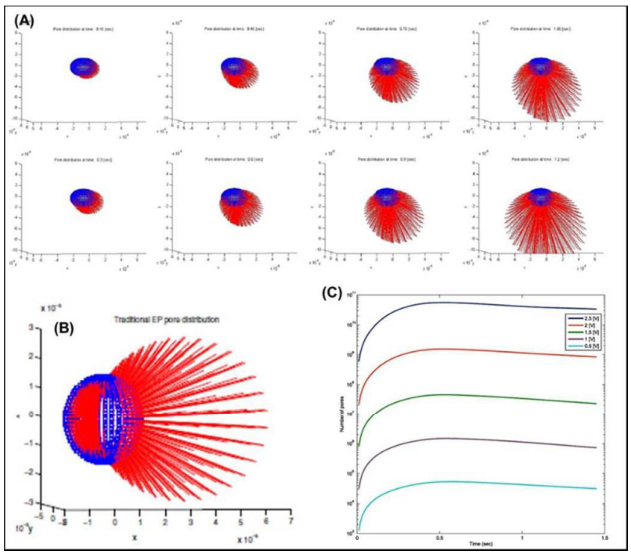

Fig. 6 Numerical simulations of single cell electroporation in MEP devices (A) Radiation-plots show the formed nano-pores are mainly distributed on the bottom hemisphere of the cell when both electrodes are placed on the bottom side of the microchannel. In contrast, (B) the nano-pore distribution becomes more homogeneous when the electrodes on both sides[94]. (C) FEM simulation shows the number of nano-pores formed on the cells as a function of the applied voltage and the time[94]. Reproduced with permission from Springer.

As discussed above, the electrode/cell configuration plays a major role in determining the outcome of MEP-based processes. Such configuration is fundamentally different in MEEP vs. MFEP systems, with MEEP devices typically allowing closer contact between the cell and electrode system. An example of this is shown in Fig. 7A[57]. FEM analysis of this system indicated that the porating electric field mainly focused on the portion of the cell that is inside the microchannel (Fig. 7B)[57]. Fei *et al* developed a micro-nozzle-based MEP platform where electric field focusing occurs mostly around the converging nozzle areas (Fig. 7C). Such shape is also expected to enhance electrophoresis-mediated cargo delivery [58]. Studies by Ionescu-Zanetti *et al.* found that electrophoresis could significantly reduce the time needed for successful cargo delivery into the cell[60].

Finally, joule heating and pH changes could significantly alter the outcome of MEP-based experiments[72]. For example, studies using temperature sensitive dyes (Rhodamin B) in MFEP devices showed that under a high electric field (800 V/cm) and with low flow rate (< 2.13 µL/min) the local temperature could reach cytotoxic levels of up to 45˚C. Other groups studied the effects of pH changes in cell viability[48], and they found that the pH values could range between 3 and 10 around the anode and cathode, respectively, with cells near the electrodes being more susceptible to death [48].

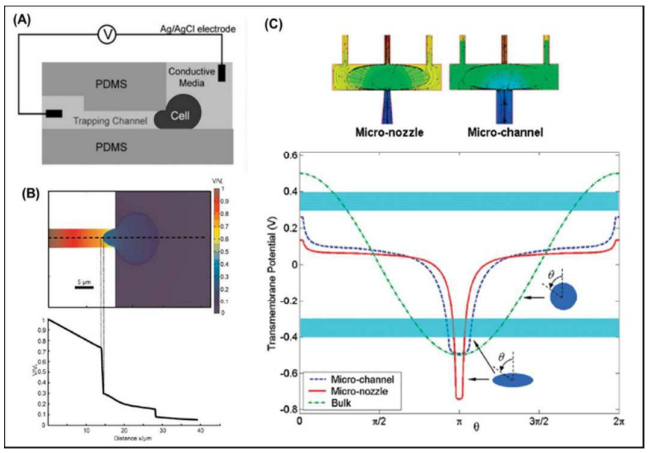

Fig. 7 MEEP-based systems and electric field distribution. (A) Schematic of a single cell trapped into a microchannel**,** which leads to (B) highly localized electroporation and the concentration of the potential drop on the cell membrane within the microchannel[57]. Reproduced with permission from RSC. (C) Electric field distribution for the micronozzle array[58]. Reproduced with permission from ACS.

4 Nano-scale electroporation systems

Further miniaturization of the electroporation systems has enabled advanced functionalities compared to BEP- or MEP-based setups. Nano-electroporation (NEP) systems, for example, focus the porating electric field on a considerably smaller (*i.e.,* nanosized) portion of the cell membrane, which results in the development of a much larger Δ_m while causing minimum to negligible damage to the cell. Here we will go over a number of representative NEP-type systems, and discuss manufacturing, theoretical and experimental aspects.

4.1 NEP-based systems

A number of NEP-based systems have been developed over the years, including (i) two-dimensional (2D) nano-channel electroporation[96-98]; (ii) nano-straw / nano-spike electroporation [99-101]; (iii) nano-wire / nano-electrode electroporation[102-104], (iv) nano-probe (or nanofountain-probe) electroporation [105, 106]; and (v) three-dimensional (3D) nano-channel electroporation[107]. Our lab was the first ones to develop an NEP-based system for efficient cell transfection[96]. The basic functional unit of this first generation device consisted of a nanochannel (90 nm in diameter, 3 µm long) interconnecting two microchannels (Fig. 8). These devices were fabricated through a simple replica molding process from lithographically-fabricated polydimethylsiloxane (PDMS) masters with stretched/combed DNA strands that ultimately gave rise to the nanochannels (Fig. 8A)[96]. Single cells were then loaded into each microchannel, in close contact with the nanochannel output, while the juxtaposing microchannel was filled with the cargo (*e.g.,* DNA, RNA, etc.) solution to be delivered (Fig. 8B)[96]. A pulsed electric field (150-350 V, 2-10 ms pulses) was subsequently applied across the nanochannel, which induced nanoscale-sized membrane permeabilization immediately followed by electrophoretic cargo delivery into the cytosol. Single-cell resolution dose control could be achieved by modulating the pulse length.

One unique advantage of NEP-based transfection is that cytosolic cargo delivery is entirely modulated by electrophoretic forces. BEP- or MEP-based approaches are still heavily dependent by downstream processes such as diffusion and/or endocytosis. Electrophoresis-based delivery facilitates the transduction of bulky cargo, such as large polycistronic plasmids encoding for multiple genes (*e.g., Oct4, Sox2, Klf4* and *cMyc* or OSKM). Such cargo is difficult to deliver with BEP- or MEP-mediated transfection[98].

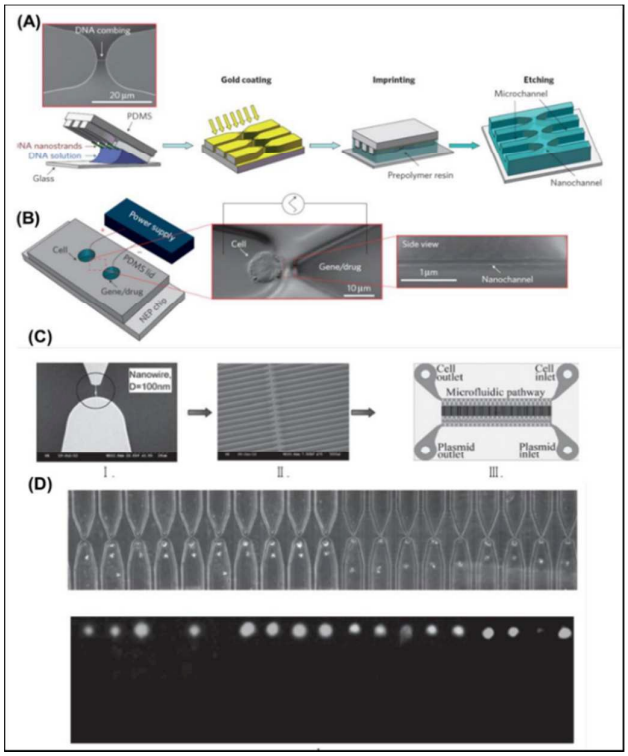

Fig. 8 2D NEP. (A) Fabrication process of NEP devices. (B) Assembly and operation of 2D NEP devices. Single cells were precisely positioned against the nanochannel outlet via optical tweezers[96]. (C) PDMS/DNA master and replica-molded device. (D) Cells loaded into the microchannels before (top) and after (bottom) delivery of OSKM plasmids[98]. Reproduced with permissions from Nature and Wiley, respectively.

The first generation of NEP devices was based on a 2D system with a limited throughput. To increase the yield, we developed 3D NEP systems (Fig. 9) that could simultaneously transfect tens of thousands to hundreds of thousands of cells in a controlled and benign manner[107]. In this case, 3D nanochannel (300-600 nm in diameter, 10 μm long) arrays are created in Si or polymers, either by combining projection and contact lithography with deep reactive ion etching (DRIE) (Fig. 9B), or by lithographically patterning a nanochanneled track etched membrane. Such systems can achieve transfection efficiencies and cell viabilities of approximately 90% and 100%, respectively, with minimum cell-to-cell variations in the transfection extent.

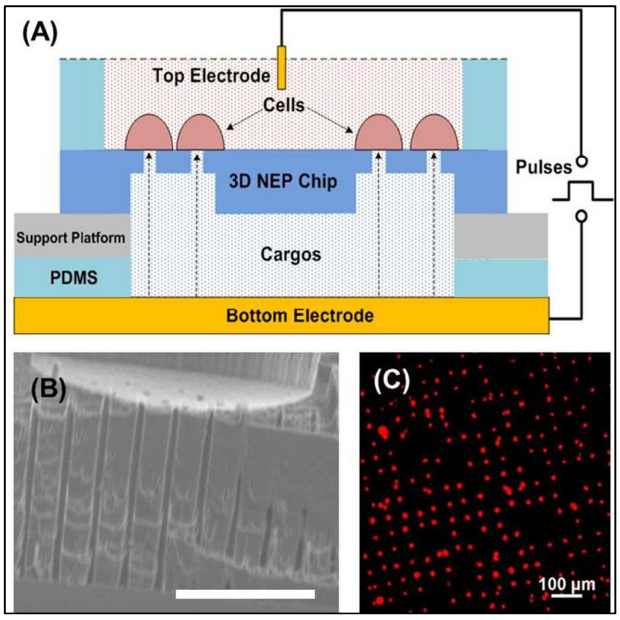

Fig. 9 Si-based 3D NEP platform for high-throughput cell transfection. (A) Schematic of the 3D NEP system[107]. (B) Cross-section micrograph. (C) Intracellular fluorescence dye expression after electro-injection through nanochannel array. Reproduced with permission from RSC.

Espinosa *et al* developed a nano-fountain probe electroporation (NFP-E) system for *in situ* cell transfection[105]. This system consists of a hollow atomic force microscopy (AFM) probe with a ~800 nm outlet that modulates membrane poration and cargo delivery (Fig. 10A, B)[105]. An automation stage is used to achieve selective single-cell transfection. Moreover, the resolution of the system allows localized transfection of a specific region on the cell. This system, however, can only handle a limited number of cells. Melosh *et al.*, on the other hand, introduced a novel nanostraw-electroporation platform based on randomly-arrayed hollow nanotubes (200 nm in diameter and 1.5 μm in height) (Fig. 10 C, D)[99]. Such structures were etched out of an alumina coated track-etched polycarbonate membrane to create a direct pathway for the delivery of a wide variety of cargo into cells, with efficiencies ranging between 81% and >90% depending on the cargo. Cellular engulfment of the nanostructures provides tight contact, often times enabling transfection to occur at no- or low voltages. By using this nano-fountain probe electroporation system, they have successfully delivered protein and DNA into cells. (ref 89)

In addition to nanochannel-, nanofountain-, or nanostraw-based electroporation, other groups have developed myriad of nanoscale components (*e.g.,* electrodes, nanowires, etc.) to further study the electroporation process (Fig. 10E, F), and define optimum voltage and/or frequency ranges to achieve reversible vs. irreversible membrane poration[104].

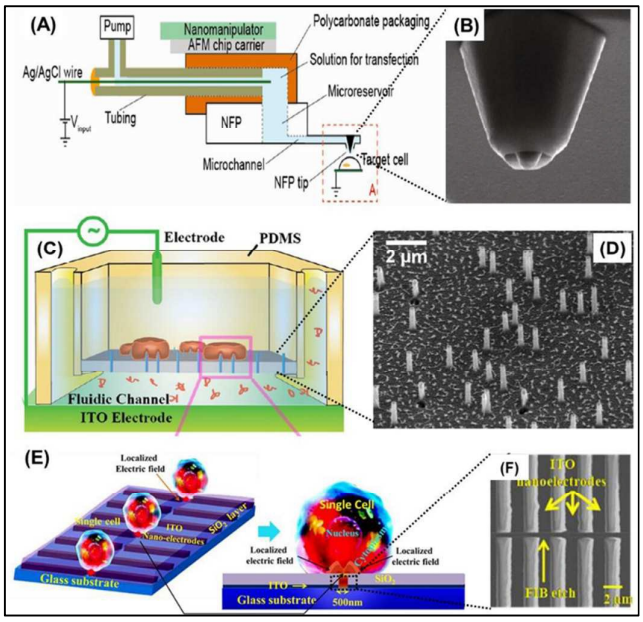

Fig. 10 Additional nanoscale electroporation systems. (A) Schematic and (B) electronic micrograph of the NFP-E platform[105]. Reproduced with permission from ACS. (C) Electroporation-based gene delivery facilitated through (D) nanostraws.[99]. Reproduced with permission from ACS. (E) Single cell electroporation by parallel nano-electrodes. (F) Electronic micrograph of the ITO nano-electrodes[104]. Reproduced with permission from AIP.

4.2 Theoretical analysis of NEP

FEM has been recently used to study multiple aspects of the NEP process[96, 100, 103-105, 107]. Such models typically represent the cell membrane as a resistor and a capacitor in parallel[96, 105]. Once a porating voltage is applied, most of the drop (~95%) occurs across the nanochannel, which has an ohmic resistance value several orders of magnitude higher compared to the cell (*e.g.,* hundreds of MΩ compared to <1 MΩ) (Fig. 8B)[107]. As such, the electrical stimuli (Δ_m) modulating membrane poration is mostly focused around the cell-nanochannel outlet interface (within <1 µm, Fig. 11A). Δ_m, at the same time, is extremely sensitive to the gap distance between the cell and the nanochannel outlet, with shorter distances resulting in higher Δ_m values[96, 107].

In addition to promoting highly focused and enhancedΔ_m, nanochannel-based poration also enables fast and efficient direct cargo delivery into the cytosol by electrophoresis. Electrophoretic forces are enhanced within the nanochannel due to the high voltage drop, which allows cargo delivery to occur within microseconds compared to diffusion-dominated processes, which could take much longer time (*e.g.,* BEP, MEP) (Fig. 11B). Experiments with quantum dots confirmed an electrophoresis-driven speed of about 490 µm/ms within a nanochannel, which is ~ 3000 times higher than the velocity within a microchannel-based system[96].

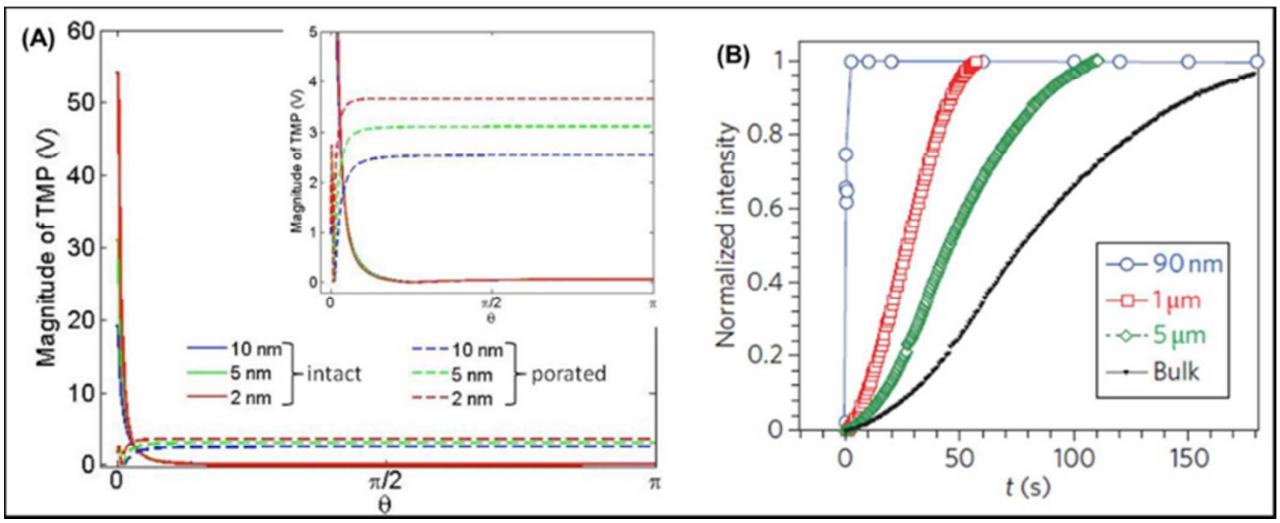

Fig. 11 Numerical simulation of the transmembrane potential, and delivery time in NEP (90 nm), BEP and MEP (1 and 5 µm). (A) Transmembrane potential distribution and intensity with respect of the gap distance between the cell and nanochannel outlet. (B) Delivery time for PI dye in NEP (blue), MEP with 1µm (red) and 5 µm channel (green), and BEP (black)[96]. Reproduced with permission from Nature.

5 Biomedical applications of micro-/nano-scale electroporation

A number of recent studies have focused on the use of miniaturized (*i.e.,* micro- to nanoscale) electroporation systems for biomedical applications, including adoptive immunotherapy, gene/RNA-based therapies, cell reprogramming, and intracellular biointerrogation of living cells, among others. Electroporation-based methods are compatible with a host of cargo, ranging from genes to proteins or protein complexes, and thus have the potential to enable a multitude of applications. Here we will discuss some of the most relevant breakthroughs in this area.

5.1 Gene therapy

Gene therapy is a simple yet revolutionary concept that seeks to cure or treat diseases by modulating gene expression[108, 109]. Multiple clinical trials with improved vector technologies have shown promising results[109]. Current approaches to gene therapy, however, face a number of practical and translational hurdles, including over-dependence on viral vectors, and lack of dosage controllability. Deterministic non-viral methods are thus needed to facilitate the transition from the lab bench to the clinic of highly promising gene therapies[110]. Miniaturized electroporation techniques, especially NEP, are poised to significantly impact this field. One area that has attracted a great deal of attention is DNA vaccination, which has been shown to modulate immune responses via delivery of plasmids genes that encode for specific antigens[111]. Electroporation-based approaches have been reported to significantly enhance DNA vaccination[112, 113]. In this section we will review some of the most relevant studies on the use of miniaturized electroporation approaches for gene therapy.

Adoptive Immunotherapy. Therapies aimed at increasing the immune system's ability to combat specific conditions have shown extremely promising results[114, 115]. Genetically-engineered immune cells (*e.g.,* T cells, NK cells), for example, have been used/studied to enhance anti-tumoral immunity, vaccine efficacy, and to modulate graft-versus-host-disease[103, 104, 116, 106]. Nevertheless, immune cell engineering still depends heavily on viral vectors that could hamper clinical implementation. Moreover, immune cells are exceedingly difficult to transfect with conventional non-viral methods such as BEP or nanocarriers[117-120]. We have implemented dielectrophoresis-assisted 3D NEP (pDEP-NEP)[121] platform for non-viral immune cell engineering. Experiments with plasmids encoding for the chimeric antigen receptor (CAR), which has been reported to enhance anti-tumoral activity in immune cells, showed that the pDEP-NEP achieved transfection efficiencies and cell viabilities around >70% and 90%, respectively (Fig. 12). Conventional BEP, on the other hand, led to transfection efficiencies of <30%, and cell viabilities around 60-70%. In addition, cell-to-cell variability was minimized considerably for pDEP-NEP compared to BEP, which suggests that NEP-based transfection yields more uniformly-engineered and possibly predictable/safer cells, which is highly important for clinical translation. Since adoptive immunotherapy requires permanent transfection of immune cells, the applicability of transient transfection by non-viral methods remains a challenge. Our preliminary data revealed that NEP delivered linear factors was able to provide a longer transfection time than ring-type plasmids delivered by BEP (data not shown). However, more effort is needed in this area.

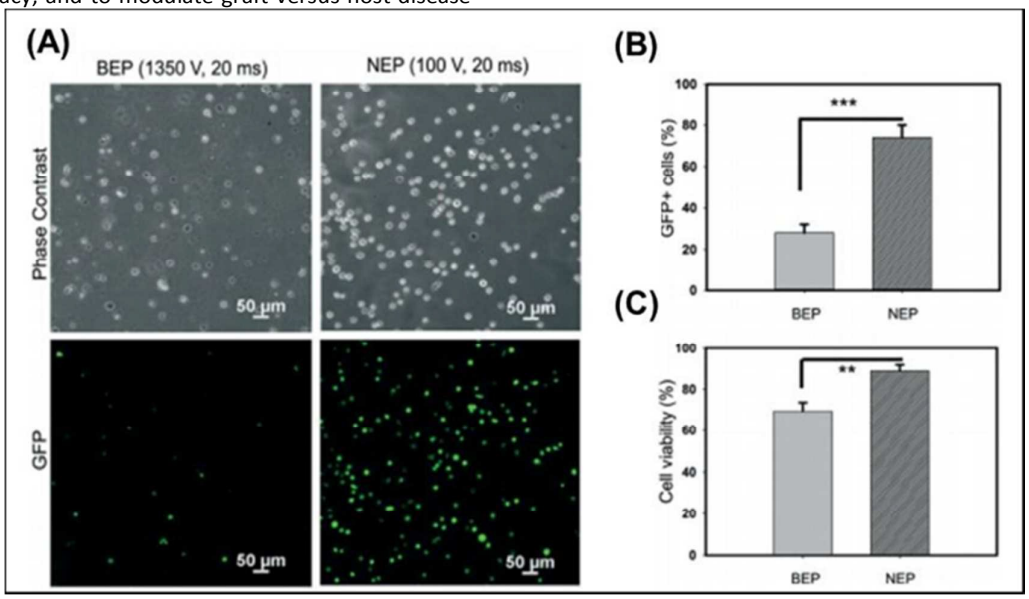

Fig.12. Safe and efficient NK cell transfection with chimeric antigen receptor (CAR) plasmids by pDEP-NEP[121]. (A) Phase contrast and epifluorescence images of NK cells 10 h after BEP- and NEP-based transfection of CAR plasmids with GFP as reporter gene. Positive epifluorescence signal represent successful expression of CAR gene. (b) Efficiency of CAR plasmid delivery and expression was significantly improved in NEP compared to BEP. ***$p < 0.005$. (C) Cell viability percentages in NEP and BEP. **$p< 0.01$. Reproduced with permission from RSC.

RNA interference (RNAi) – based Therapy. Gene expression for therapeutic applications can also be modulated by transfecting a specific RNAi[122, 123, 124]. Such concept has shown great promise for the treatment of a number of diseases, including cancer. Small interfering RNA (siRNAs) or microRNAs (miRNAs) have been used, for example, to successfully regulate oncogene or proto-oncogene expression (*e.g., VEGF*, *KSP*) in clinical trials for liver cancer[125]. Successful delivery of siRNA or miRNA is the key to efficacious RNAi-based therapeutics[125]. Although nanocarriers have been widely used to deliver RNAis into cells, such approach presents numerous limitations, including stochastic delivery, size uniformity, aggregation, low loading capacity/efficiency, and poor stability and biocompatibility[121, 126]. Recent reports have highlighted the potential of NEP-based transfection for the development of RNAi-assisted therapies. The ability to deliver siRNAs in a

dose- and time-controlled manner at the single cell level allowed for the determination of optimum pro-apoptotic strategies for the potential treatment of acute myeloid leukemia (Fig. 13 A, B)[127].

Gene Editing. Making precise genetic modifications to the living cells has long fascinated bioengineering researchers. Electroporation is found to be frequently utilized in gene editing applications for vector delivery. The CRISPR-Cas9 systems (Clustered Regularly Interspaced Short Palindromic Repeats (CRISPR)—Cas9, a CRISPR-associated protein) recently emerged as a potentially potent genome editing tool in molecular biology. Here we briefly review recent electroporation-involved works associated with CRISPR/Cas9 gene editing method. Maresch *et al.* demonstrated that by electroporation-based multiplexed delivery of CRISPR/Cas9 into mice pancreatic cells, "simultaneous editing" of a number of gene sets in single living cells was realized[128] (Fig. 13C). Their data pointed out that CRISPR/Cas9 will carry out several tasks, ranging from combinatorial gene-network analysis, *in vivo* synthetic lethality screening, to chromosome engineering. Chu *et al.* also presented that enhancing homology-directed repair (HDR) improved the efficiency of CRISPR-Cas9-induced precise gene editing[129]. However, it is worth to note that most of these works pioneering the research of gene editing are heavily dependent on bulk electroporation, which leads to stochastic and harsh environment to cells *in vivo*. Therefore, it provides great opportunities to MEP and NEP for study of CRISPR-Cas9 and other gene editing approaches in more deterministic, real-time and safer manner in the future.

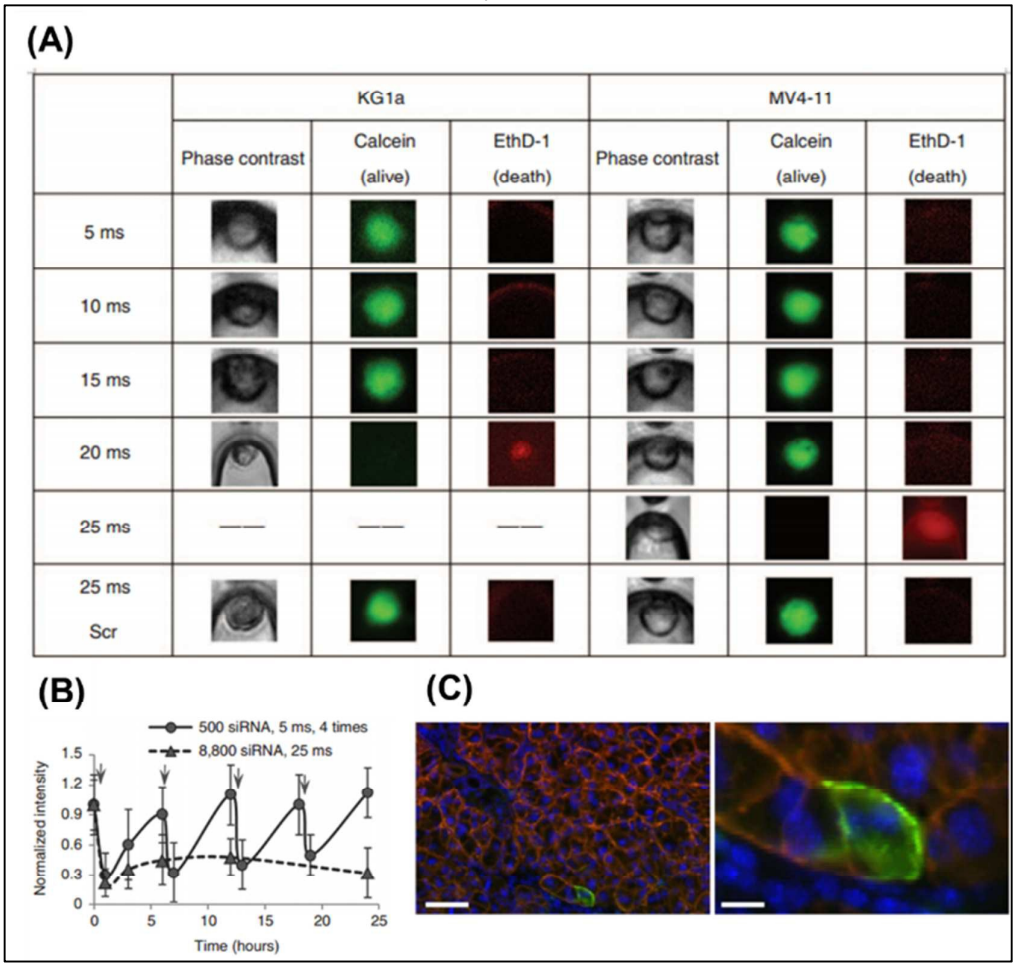

Fig. 13. RNA interference therapy and gene editing. (A) NEP-based *Mcl-1* siRNA therapy in wild-type and FLT3-ITD AML Cells using different NEP conditions. Live/dead cell staining was used to determine critical dosing to induce cell death. (B) Changes in *Mcl-1* expression with different siRNA doses[127]. (C)Transition of membranous red to cytoplasmic/ membranous green fluorescence in electroporation-transfected acinar cells[128]. Scale bars, 50 µm (left) and 10 µm (right). Reproduced with permission from Wiley and Nature, respectively.

5.2 Regenerative medicine

Many disease conditions are typically caused by quantitative and/or functional deficiencies in specific cell types. The goal of regenerative medicine is thus to replace lost structures and/or functions that result from such deficiencies. Recent advances in nuclear reprogramming (*e.g.,* Induced Pluripotent Stem Cells or iPSCs)[130] have been a great leap forward in regenerative medicine research, especially direct nuclear reprogramming[118, 123], where cells can transdifferentiate directly into the cell of interest without passing through an iPSC stage. Exploiting the full potential of nuclear reprogramming, however, requires precise and timely delivery of complex combinations of reprogramming genes, which cannot be accomplished

efficiently with current transfection methodologies due to their highly stochastic nature. The inability to control these factors could lead to inefficient and/or potentially unsafe reprogramming outcomes.

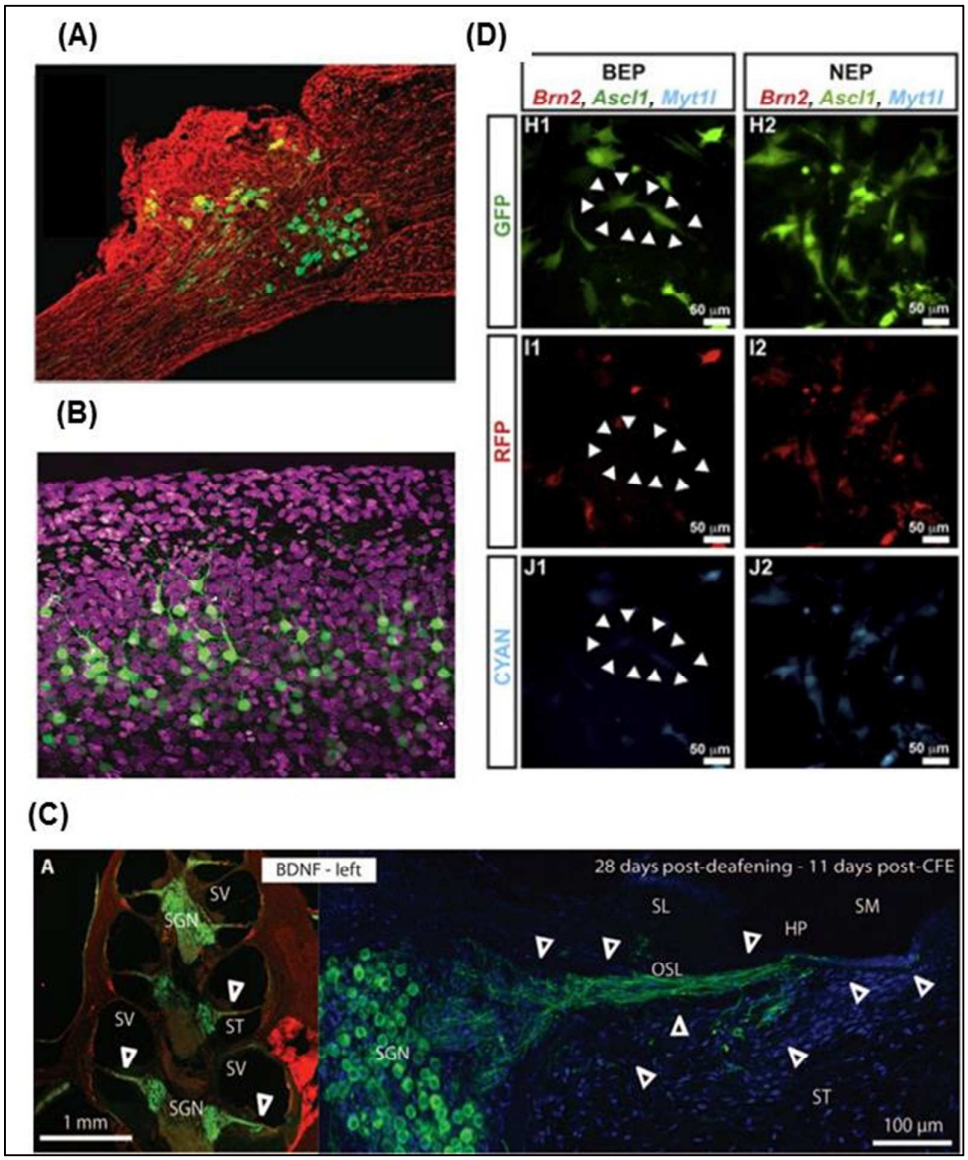

Fig. 14. Recent mice/nanoscale electroporation applications in regenerative medicine. (A) Fluorescent images of an EGFP-transfected dorsal root ganglion (DRG) immunostained with the neuronal marker βIII tubulin (red)[131]. Reproduced with permission from Nature. (B) Confocal images of representative fields from coronal hippocampal with electroporated cells (green). scale bars, 100 µm[132]. Reproduced with permission from Nature. (C) Representative immunofluorescence image showing that "close-field" electroporation (CFE) mediates BDNF gene therapy in deafened guinea pig cochleae[133]. Reproduced with permission from AAAS. (D) comparison between BEP- and NEP-based delivery of *Ascl1*, *Brn2*, and *Myt1l* (color coded green, red, and blue) plasmids into MEFs[126]. Reproduced with permission from Elsevier.

Saijilafu *et al.* presented neuron regeneration work using an efficient *in vivo* electroporation technique enabling accurate and precise manipulation of gene expression[131]. They demonstrated this method successfully transfected adult dorsal root ganglion (DRG) neurons (Fig. 14A), and thus genetically dissect axon injury and regeneration models. Cancedda group presented a novel *in utero* electroporation technique based on triple-electrode configuration which firstly transfected Purkinje cells in the rat brain areas (Fig. 14 B), which had not been achieved before[132]. The *in utero* configuration is promising to provide new insight into neuronal plasticity, and can be applied into other tissues including skin and cardiac tissue. Pinyon *et al.* introduced a novel close-field electroporation (CFE) with cochlear implant electrode, by which they for the first time improved the performance of "bionic ear" by enhancing neural interface via brain-derived neurotrophic factor (BDNF) delivery (Fig. 14 C)[133].

Most of these electroporation devices are relied on the bulk electroporation. We have developed a novel and yet simple to implement approach to transfect and directly reprogram large

numbers of cells in an NEP-like fashion[126]. Deterministic NEP-based delivery of *ABM* (*Ascl1*, *Brn2*, and *Myt1l*) (Fig. 14D) not only resulted in significantly improved reprogramming efficiencies compared to BEP, but also allowed us to uncover a number of stochastic barriers to the reprogramming process, including the potential roles the of *Ascl1* dosage and the S-phase cyclin CCNA2.

5.3 *In situ* intracellular probing

Disease onset and progression is typically driven by subtle but critical changes in intracellular activity that are often elusive to conventional cell analysis techniques[134, 135, 129, 130]. Novel technologies are thus needed to enable a more thorough monitoring of cellular activity both in real time and at the single cell level[131, 132].

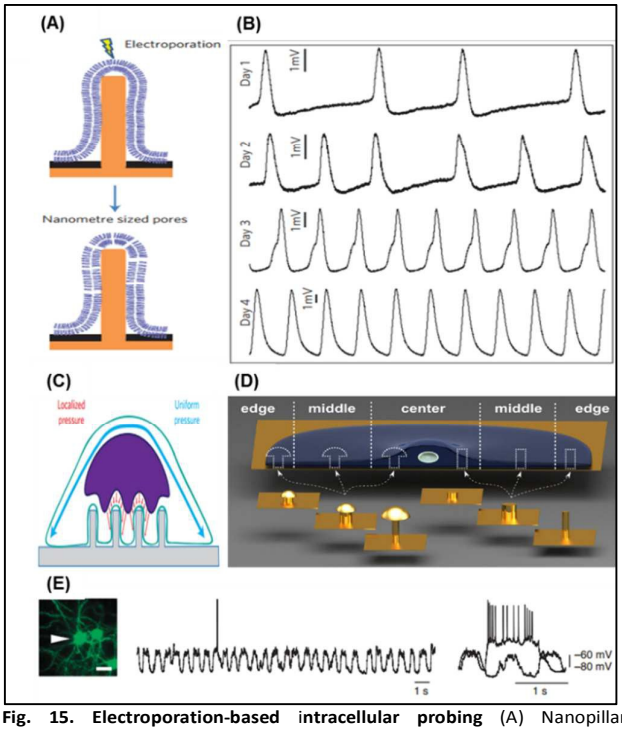

Fig. 15. Electroporation-based intracellular probing (A) Nanopillar electrode device for intracellular recording of action potentials. (B) Action potentials could be recorded for over four consecutive days at the single cell level[136]. Reproduced with permission from Nature. (C) Vertical nanopillars for probing of nuclear biomechanics[137]. Reproduced with permission from Nature. (D) Schematic diagram illustrating the interface between the nanostructures and cells[138]. Reproduced with permission from ACS. (E) *In vivo* single living cell probe of a neuron 24 h after electroporation. Left, cells with GFP fluorescence were electroporated; arrowhead indicates the cell recorded. Middle, real-time recording of membrane potential fluctuations and action potentials. Right, responses to current injections of 350 pA and -100 pA. Scale bars, 20 μm[139]. Reproduced with permission from Nature.

Xie *et al.* developed a vertical nano-pillar electroporation device for recording intracellular action potentials in living cardiomyocytes *in vitro* (Fig. 15 A)[136]. Intracellular recordings were successfully collected on HL-1 cells over a period of four consecutive days (Fig. 15 B). Hanson *et al*. used a similar approach to characterize nuclear biomechanics in adherent cells (Fig. 15 C)[137]. This versatile nanopillar electroporation-recording platform could find applications in drug discovery with electrogenic cells, and/or cancer research among other things. Santoro *et al*. carried out a more in-depth study of the interface between 3D nano-electrode structures and cells[138] (Fig. 15 D). In additional, a single-cell electroporation and *in situ* recording device has been presented for labeling neurons by Kitamura *et al*., which enables the recording, labeling and genetic manipulation of single neurons *in vivo* (Fig. 15 E)[139].

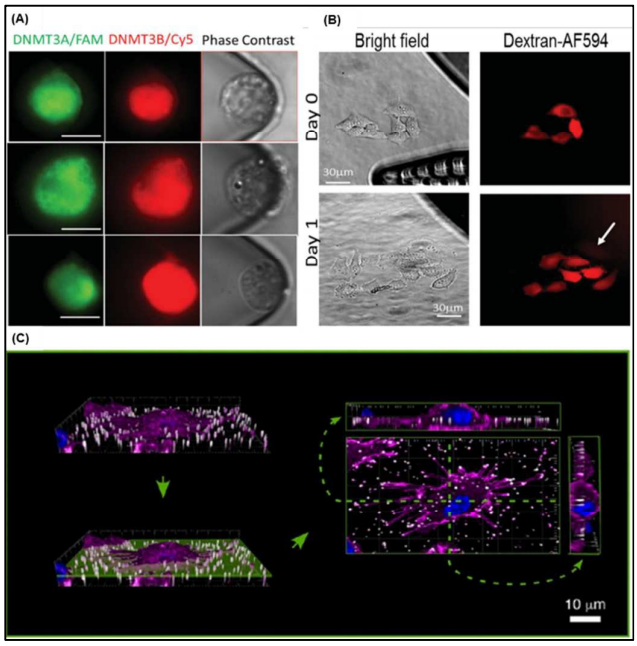

Fig. 16. Nano-electroporation for living cell interrogation by benign detection and perturbation at RNA level (A) micrographs of wild-type Kasumi-1 AML cells transfected with DNMT3A/B MBs[97]. Reproduced with permission from Wiley. (B) HeLa cells transfected with MBs and imaged after a 24 h incubation (day 1) showing that the electroporated cells divided[140]. Reproduced with permission from Wiley. (C) Three-dimensional reconstruction (left) of confocal images of mouse bone marrow derived dendritic cell (BMDC) (membrane: magenta, nucleus: blue) on top of Alexa-labeled NWs (white)[141]. Reproduced with permission from ACS.

Zhao *et al.* used 2D NEP to conduct intracellular probing of living AML cells (Fig. 16 A) via controlled timed delivery of molecular beacons (MBs)[97]. Giraldo-Vela *et al.* also used MBs in combination with nanofountain-based electroporation to detect mRNA at the single-cell level (Fig. 16 B)[140]. Finally, Shalek *et al*. used nanowire-based delivery of siRNAs to conduct *ex vivo* biointerrogation of immune cells (Fig. 16 C) [141]. In addition to the biosensors based on nucleic acids, fluorescent biosensors in the form of proteins have also been successfully delivered via electroporation[88]. Fluorescence resonance energy transfer (FRET)-based protein biosensors have the potential to monitor the dynamics of protein (*e.g.,* Src) activity with excellent spatiotemporal resolution. Electroporation-assisted intracellular probing can be achieved not only by deploying various biosensors into the living cells, but also by extracting biomolecules of interest from the cells. Lu's Group developed a series of microfluidic-based electroporation systems to selectively extract proteins and genes from mammalian cells and bacterial[89, 142].

6 Additional applications of micro-/nano-scale electroporation

In addition to biomedical applications, electroporation has been utilized in a variety of disciplines, including the food industry, and microbiology. For instance, pulsed electric fields (PEF) electroporation has been reported to significantly improve microorganism inactivation efficiency compared with traditional thermal pasteurization methods[143, 144]. PEF has also been used in the in food processing to induce cell wall breakdown, which facilitates extraction processes from plant cells. For additional discussion on this topic, the reader is referred to more comprehensive reviews on this matter[144-146].

7 Conclusions and Outlook

Micro- and nanoscale technologies have played a fundamental role in the development of advanced non-viral transfection approaches for numerous fundamental and translational applications. Microscale electroporation offers multiple advantages over conventional bulk electroporation approaches, while further miniaturization (*i.e.,* nanoscale-based electroporation) has enabled a host of additional capabilities including dosage control and causing minimum to negligible cell perturbation. Although micro/nano-electroporation platforms hold great promise, it should be noted that most systems require significant expertise and resources from a manufacturing and/or operation stand point, which could hamper widespread use of these technologies. Further research needs to be conducted in order to develop easily scalable fabrication processes, as well as more user friendly operation protocols.

Altogether, micro/nanoscale electroporation approaches are poised to significantly impact both biomedical research and clinical medicine, and as such, warrant further study and proper allocation of resources for successful development. For example, current micro/nanoscale electroporation can successfully deliver cargo into the cytosol, but many gene therapy applications require cargo to be transported into nucleus for permanent transfection or specific functions. Design of 'nucleus-target', instead of 'naked' cargo, in combination of efficient electroporation platforms will be highly valuable. There is also great potential to apply *in vivo* MEP / NEP systems for personalized cell therapy, regenerative medicine and gene editing.

Acknowledgements

The authors are grateful to the National Science Foundation (EEC-0914790) for the financial support of this study.

Notes and references

1. P. D. Hsu, E. S. Lander and F. Zhang, *Cell*, 2014, **157**, 1262-1278.
2. J. A. Doudna and E. Charpentier, *Science*, 2014, **346**, 1077-+.
3. L. Koch, *Nat Rev Genet*, 2016.
4. N. P. Restifo, M. E. Dudley and S. A. Rosenberg, *Nat Rev Immunol*, 2012, **12**, 269-281.
5. Y. Buganim, D. A. Faddah and R. Jaenisch, *Nat Rev Genet*, 2013, **14**, 427-439.
6. J. B. Gurdon, *Nat Rev Mol Cell Bio*, 2016, **17**, 137-138.
7. A. El-Sayed and H. Harashima, *Mol Ther*, 2013, **21**, 1118-1130.
8. S. Mitragotri, *Adv Drug Deliver Rev*, 2013, **65**, 100-103.
9. S. N. Wang and L. J. Lee, *Biomicrofluidics*, 2013, **7**.
10. T. Geng and C. Lu, *Lab Chip*, 2013, **13**, 3803-3821.
11. P. E. Boukany, A. Morss, W. C. Liao, B. Henslee, H. Jung, X. Zhang, B. Yu, X. Wang, Y. Wu, L. Li, K. Gao, X. Hu, X. Zhao, O. Hemminger, W. Lu, G. P. Lafyatis and L. J. Lee, *Nat Nanotechnol*, 2011, **6**, 747-754.
12. L. Nan, Z. D. Jiang and X. Y. Wei, *Lab Chip*, 2014, **14**, 1060-1073.
13. T. Kotnik, W. Frey, M. Sack, S. H. Meglic, M. Peterka and D. Miklavcic, *Trends Biotechnol*, 2015, **33**, 480-488.
14. Z. G. Yang, L. Q. Chang, C. L. Chiang and L. J. Lee, *Curr Pharm Design*, 2015, **21**, 6081-6088.
15. E. Neumann, M. Schaefer-Ridder, Y. Wang and P. H. Hofschneider, *The EMBO Journal*, 1982, **1**, 841-845.
16. T. Santra and F. Tseng, *Micromachines*, 2013, **4**, 333.
17. J. Gehl, *Acta Physiologica Scandinavica*, 2003, **177**, 437-447.
18. T. Kotnik, P. Kramar, G. Pucihar, D. Miklavcic and M. Tarek, *IEEE Electrical Insulation Magazine*, 2012, **28**, 14-23.
19. S. Haberl, D. Miklavcic, G. Sersa, W. Frey and B. Rubinsky, *IEEE Electrical Insulation Magazine*, 2013, **29**, 29-37.
20. M. Reber, ek, D. Miklav, C. Bertacchini and M. Sack, *IEEE Electrical Insulation Magazine*, 2014, **30**, 8-18.
21. J. C. Weaver, *IEEE Transactions on Dielectrics and Electrical Insulation*, 2003, **10**, 754-768.
22. T. Y. Tsong, *Biophysical Journal*, 1991, **60**, 297-306.
23. S. Y. Ho and G. S. Mittal, *Critical Reviews in Biotechnology*, 1996, **16**, 349-362.
24. J. C. Weaver and Y. A. Chizmadzhev, *Bioelectrochemistry and Bioenergetics*, 1996, **41**, 135-160.
25. R. Davalos, Y. Huang and B. Rubinsky, *Microscale Thermophysical Engineering*, 2000, **4**, 147-159.
26. E. Neumann, S. Kakorin and K. Tœnsing, *Bioelectrochemistry and Bioenergetics*, 1999, **48**, 3-16.
27. R. Stämpfli, *An. Acad. Bras. Cienc.*, 1958, **30**, 57-63.
28. G. Narayanan and M. H. Doshi, *Curr Urol Rep*, 2016, **17**, 15.
29. C. Mansson, R. Brahmstaedt, A. Nilsson, P. Nygren and B. M. Karlson, *Eur J Surg Oncol*, 2016.
30. Y. Zu, S. Huang, W.-C. Liao, Y. Lu and S. Wang, *Journal of biomedical nanotechnology*, 2014, **10**, 982-992.
31. D. Zhao, D. Huang, Y. Li, M. Wu, W. Zhong, Q. Cheng, X. Wang, Y. Wu, X. Zhou, Z. Wei, Z. Li and Z. Liang, *Scientific Reports*, 2016, **6**, 18469.
32. F. Kashanchi, J. F. Duvall and J. N. Brady, *Nucleic Acids Res*, 1992, **20**, 4673-4674.
33. S. O. Choi, Y. C. Kim, J. W. Lee, J. H. Park, M. R. Prausnitz and M. G. Allen, *Small*, 2012, **8**, 1081-1091.
34. W. B. Wang, P. M. Kutny, S. L. Byers, C. J. Longstaff, M. J. DaCosta, C. H. Pang, Y. F. Zhang, R. A. Taft, F. W. Buaas and H. Y. Wang, *J Genet Genomics*, 2016, **43**, 319-327.
35. S. Remy, V. Quillaud-Chenouard, L. Tesson, S. Menoret, C. Usal, L. Brusselle, T. H. Nguyen, A. De Cian, C. Giovannangeli, J. P. Concordet and I. Anegon, *Transgenic Res*, 2016, **25**, 258-258.
36. Y.-C. Lin, C.-M. Jen, M.-Y. Huang, C.-Y. Wu and X.-Z. Lin, *Sensors and Actuators B: Chemical*, 2001, **79**, 137-143.

37. L. Chang, J. Hu, F. Chen, Z. Chen, J. Shi, Z. Yang, Y. Li and L. J. Lee, *Nanoscale*, 2016, **8**, 3181-3206.
38. S. Wang and L. J. Lee, *Biomicrofluidics*, 2013, **7**, 011301.
39. M. B. Fox, D. C. Esveld, A. Valero, R. Luttge, H. C. Mastwijk, P. V. Bartels, A. Berg and R. M. Boom, *Analytical and Bioanalytical Chemistry*, 2006, **385**, 474-485.
40. W. G. Lee, U. Demirci and A. Khademhosseini, *Integrative Biology*, 2009, **1**, 242-251.
41. S. Movahed and D. Li, *Microfluidics and Nanofluidics*, 2010, **10**, 703-734.
42. M. Wang, O. Orwar, J. Olofsson and S. G. Weber, *Analytical and Bioanalytical Chemistry*, 2010, **397**, 3235-3248.
43. J. Olofsson, K. Nolkrantz, F. Ryttsén, B. A. Lambie, S. G. Weber and O. Orwar, *Current Opinion in Biotechnology*, 2003, **14**, 29-34.
44. Y. Huang and B. Rubinsky, *Biomedical Microdevices*, 1999, **2**, 145-150.
45. Y. Huang and B. Rubinsky, *Sensors and Actuators A: Physical*, 2001, **89**, 242-249.
46. H. Huang, Z. Wei, Y. Huang, D. Zhao, L. Zheng, T. Cai, M. Wu, W. Wang, X. Ding, Z. Zhou, Q. Du, Z. Li and Z. Liang, *Lab on a Chip*, 2011, **11**, 163-172.
47. P. Deng, H. Mei and Y. K. Lee, 2014.
48. Y. Li, M. Wu, D. Zhao, Z. Wei, W. Zhong, X. Wang, Z. Liang and Z. Li, *Scientific Reports*, 2015, **5**, 17817.
49. F. Kupfer, S. M. Lattanzio, M. Maschietto, A. Botos, M. Mahnkopf, J. Bruns, M. Schreiter, S. Vassanelli and R. Thewes, 2015.
50. Y.-C. Lin, M. Li and C.-C. Wu, *Lab on a Chip*, 2004, **4**, 104-108.
51. Y. Xu, S. Su, C. Zhou, Y. Lu and W. Xing, *Bioelectrochemistry*, 2015, **102**, 35-41.
52. I. Zudans, A. Agarwal, O. Orwar and S. G. Weber, *Biophysical Journal*, 2007, **92**, 3696-3705.
53. Y. Huang and B. Rubinsky, *Sensors and Actuators A: Physical*, 2003, **104**, 205-212.
54. J. A. Lundqvist, F. Sahlin, M. A. I. Åberg, A. Strömberg, P. S. Eriksson and O. Orwar, *Proceedings of the National Academy of Sciences*, 1998, **95**, 10356-10360.
55. K. Nolkrantz, C. Farre, A. Brederlau, R. I. D. Karlsson, C. Brennan, P. S. Eriksson, S. G. Weber, M. Sandberg and O. Orwar, *Analytical Chemistry*, 2001, **73**, 4469-4477.
56. A. Valero, J. N. Post, J. W. van Nieuwkasteele, P. M. ter Braak, W. Kruijer and A. van den Berg, *Lab Chip*, 2008, **8**, 62-67.
57. M. Khine, A. Lau, C. Ionescu-Zanetti, J. Seo and L. P. Lee, *Lab on a Chip*, 2005, **5**, 38-43.
58. Z. Fei, X. Hu, H.-w. Choi, S. Wang, D. Farson and L. J. Lee, *Analytical Chemistry*, 2010, **82**, 353-358.
59. W. Kang, S. S. P. Nathamgari, J. P. Giraldo-Vela, R. L. McNaughton, J. Kessler and H. D. Espinosa, 2014.
60. C. Ionescu-Zanetti, A. Blatz and M. Khine, *Biomedical Microdevices*, 2007, **10**, 113-116.
61. L. Chang, M. Howdyshell, W.-C. Liao, C.-L. Chiang, D. Gallego-Perez, Z. Yang, W. Lu, J. C. Byrd, N. Muthusamy, L. J. Lee and R. Sooryakumar, *Small*, 2015, **11**, 1818-1828.
62. Y.-C. Chung, Y.-S. Chen and S.-H. Lin, *Sensors and Actuators B: Chemical*, 2015, **213**, 261-267.
63. Y. Zhan, J. Wang, N. Bao and C. Lu, *Analytical Chemistry*, 2009, **81**, 2027-2031.
64. R. Ziv, Y. Steinhardt, G. Pelled, D. Gazit and B. Rubinsky, *Biomedical Microdevices*, 2008, **11**, 95-101.
65. S. C. Bürgel, C. Escobedo, N. Haandbæk and A. Hierlemann, *Sensors and Actuators B: Chemical*, 2015, **210**, 82-90.
66. G.-B. Lee, C.-J. Chang, C.-H. Wang, M.-Y. Lu and Y.-Y. Luo, *Microsystems & Nanoengineering*, 2015, **1**, 15007.
67. H.-Y. Wang and C. Lu, *Analytical Chemistry*, 2006, **78**, 5158-5164.
68. A. Adamo, A. Arione, A. Sharei and K. F. Jensen, *Analytical Chemistry*, 2013, **85**, 1637-1641.
69. J. Wang, M. J. Stine and C. Lu, *Analytical Chemistry*, 2007, **79**, 9584-9587.
70. H. Lu, M. A. Schmidt and K. F. Jensen, *Lab on a Chip*, 2005, **5**, 23-29.
71. Z. Wei, X. Li, D. Zhao, H. Yan, Z. Hu, Z. Liang and Z. Li, *Analytical Chemistry*, 2014, **86**, 10215-10222.
72. B. del Rosal, C. Sun, D. N. Loufakis, C. Lu and D. Jaque, *Lab on a Chip*, 2013, **13**, 3119-3127.
73. T. Geng, Y. Zhan, J. Wang and C. Lu, *Nat. Protocols*, 2011, **6**, 1192-1208.
74. J. Wang, Y. Zhan, V. M. Ugaz and C. Lu, *Lab on a Chip*, 2010, **10**, 2057-2061.
75. N. Demierre, T. Braschler, P. Linderholm, U. Seger, H. van Lintel and P. Renaud, *Lab on a Chip*, 2007, **7**, 355-365.
76. T. Geng, Y. Zhan, H.-Y. Wang, S. R. Witting, K. G. Cornetta and C. Lu, *Journal of Controlled Release*, 2010, **144**, 91-100.
77. T. Zhu, C. Luo, J. Huang, C. Xiong, Q. Ouyang and J. Fang, *Biomedical Microdevices*, 2009, **12**, 35-40.
78. Z. Wei, D. Zhao, X. Li, M. Wu, W. Wang, H. Huang, X. Wang, Q. Du, Z. Liang and Z. Li, *Analytical Chemistry*, 2011, **83**, 5881-5887.
79. D. Selmeczi, T. S. Hansen, Ö. Met, I. M. Svane and N. B. Larsen, *Biomedical Microdevices*, 2011, **13**, 383-392.
80. B. del Rosal, C. Sun, D. N. Loufakis, C. Luc and D. Jaque, *Lab Chip*, 2013, **13**, 3119-3127.
81. Y. H. Zhan, Z. N. Cao, N. Bao, J. B. Li, J. Wang, T. Geng, H. Lin and C. Lu, *J Control Release*, 2012, **160**, 570-576.
82. T. Geng, Y. H. Zhan, H. Y. Wang, S. R. Witting, K. G. Cornetta and C. Lu, *J Control Release*, 2010, **144**, 91-100.
83. H. Y. Wang and C. Lu, *Biotechnol Bioeng*, 2006, **95**, 1116-1125.
84. H. Y. Wang and C. Lu, *Anal Chem*, 2006, **78**, 5158-5164.
85. T. Geng, Y. H. Zhan, J. Wang and C. Lu, *Nat Protoc*, 2011, **6**, 1192-1208.
86. S. Ma, B. Schroeder, C. Sun, D. N. Loufakis, Z. N. Cao, N. Sriranganathan and C. Lu, *Integr Biol-Uk*, 2014, **6**, 973-978.
87. C. Sun, Z. N. Cao, M. Wu and C. Lu, *Anal Chem*, 2014, **86**, 11403-11409.
88. C. Sun, M. X. Ouyang, Z. N. Cao, S. Ma, H. Alqublan, N. Sriranganathan, Y. X. Wang and C. Lu, *Chem Commun*, 2014, **50**, 11536-11539.
89. T. Geng, N. Bao, N. Sriranganathanw, L. W. Li and C. Lu, *Anal Chem*, 2012, **84**, 9632-9639.
90. Y. H. Zhan, C. Sun, Z. N. Cao, N. Bao, J. H. Xing and C. Lu, *Anal Chem*, 2012, **84**, 8102-8105.
91. H. Lambert, R. Pankov, J. Gauthier and R. Hancock, *Biochem Cell Biol*, 1990, **68**, 729-734.
92. A. Meir and B. Rubinsky, *RSC Advances*, 2014, **4**, 54603-54613.
93. S. Movahed and D. Li, *The Journal of Membrane Biology*, 2012, **246**, 151-160.
94. A. Kaner, I. Braslavsky and B. Rubinsky, *Biomedical Microdevices*, 2013, **16**, 181-189.

95. O. T. Nedelcu, R. Corman, D. Stan and C. M. Mihailescu, 2015.
96. P. E. Boukany, A. Morss, W.-c. Liao, B. Henslee, H. Jung, X. Zhang, B. Yu, X. Wang, Y. Wu, L. Li, K. Gao, X. Hu, X. Zhao, HemmingerO, W. Lu, G. P. Lafyatis and L. J. Lee, *Nat Nano*, 2011, **6**, 747-754.
97. X. Zhao, X. Huang, X. Wang, Y. Wu, A.-K. Eisfeld, S. Schwind, D. Gallego-Perez, P. E. Boukany, G. I. Marcucci and L. J. Lee, *Advanced Science*, 2015, **2**, n/a-n/a.
98. K. Gao, L. Li, L. He, K. Hinkle, Y. Wu, J. Ma, L. Chang, X. Zhao, D. G. Perez, S. Eckardt, J. McLaughlin, B. Liu, D. F. Farson and L. J. Lee, *Small*, 2014, **10**, 1015-1023.
99. X. Xie, A. M. Xu, S. Leal-Ortiz, Y. Cao, C. C. Garner and N. A. Melosh, *ACS Nano*, 2013, **7**, 4351-4358.
100. K. Riaz, S. F. Leung, S. Tripathi, G. S. Sethi, H. Shagoshtasbi, Z. Fan and Y. K. Lee, 2014.
101. K. Riaz, S. F. Leung, H. Shagoshtasbi, Z. Fan and Y. K. Lee, 2015.
102. N. Jokilaakso, E. Salm, A. Chen, L. Millet, C. D. Guevara, B. Dorvel, B. Reddy, A. E. Karlstrom, Y. Chen, H. Ji, Y. Chen, R. Sooryakumar and R. Bashir, *Lab on a Chip*, 2013, **13**, 336-339.
103. T. S. Santra, H.-Y. Chang, P.-C. Wang and F.-G. Tseng, *Analyst*, 2014, **139**, 6249-6258.
104. T. S. Santra, P.-C. Wang, H.-Y. Chang and F.-G. Tseng, *Applied Physics Letters*, 2013, **103**, 233701.
105. W. Kang, F. Yavari, M. Minary-Jolandan, J. P. Giraldo-Vela, A. Safi, R. L. McNaughton, V. Parpoil and H. D. Espinosa, *Nano Letters*, 2013, **13**, 2448-2457.
106. J. P. Giraldo-Vela, W. Kang, R. L. McNaughton, X. Zhang, B. M. Wile, A. Tsourkas, G. Bao and H. D. Espinosa, *Small*, 2015, **11**, 2386-2391.
107. L. Chang, P. Bertani, D. Gallego-Perez, Z. Yang, F. Chen, C. Chiang, V. Malkoc, T. Kuang, K. Gao, L. J. Lee and W. Lu, *Nanoscale*, 2016, **8**, 243-252.
108. S. Hacein-Bey-Abina, J. Hauer, A. Lim, C. Picard, G. P. Wang, C. C. Berry, C. Martinache, F. Rieux-Laucat, S. Latour, B. H. Belohradsky, L. Leiva, R. Sorensen, M. Debre, J. L. Casanova, S. Blanche, A. Durandy, F. D. Bushman, A. Fischer and M. Cavazzana-Calvo, *N Engl J Med*, 2010, **363**, 355-364.
109. L. Naldini, *Nature*, 2015, **526**, 351-360.
110. C. E. Thomas, A. Ehrhardt and M. A. Kay, *Nat Rev Genet*, 2003, **4**, 346-358.
111. B. Ferraro, M. P. Morrow, N. A. Hutnick, T. H. Shin, C. E. Lucke and D. B. Weiner, *Clin Infect Dis*, 2011, **53**, 296-302.
112. M. Rosati, A. Valentin, R. Jalah, V. Patel, A. von Gegerfelt, C. Bergamaschi, C. Alicea, D. Weiss, J. Treece, R. Pal, P. D. Markham, E. T. A. Marques, J. T. August, A. Khan, R. Draghia-Akli, B. K. Felber and G. N. Pavlakis, *Vaccine*, 2008, **26**, 5223-5229.
113. L. A. Hirao, L. Wu, A. S. Khan, D. A. Hokey, J. Yan, A. L. Dai, M. R. Betts, R. Draghia-Akli and D. B. Weiner, *Vaccine*, 2008, **26**, 3112-3120.
114. W. Yang, Y. Bai, Y. Xiong, J. Zhang, S. Chen, X. Zheng, X. Meng, L. Li, J. Wang, C. Xu, C. Yan, L. Wang, C. C. Chang, T. Y. Chang, T. Zhang, P. Zhou, B. L. Song, W. Liu, S. C. Sun, X. Liu, B. L. Li and C. Xu, *Nature*, 2016, **531**, 651-655.
115. M. Caskey, F. Klein, J. C. Lorenzi, M. S. Seaman, A. P. West, Jr., N. Buckley, G. Kremer, L. Nogueira, M. Braunschweig, J. F. Scheid, J. A. Horwitz, I. Shimeliovich, S. Ben-Avraham, M. Witmer-Pack, M. Platten, C. Lehmann, L. A. Burke, T. Hawthorne, R. J. Gorelick, B. D. Walker, T. Keler, R. M. Gulick, G. Fatkenheuer, S. J. Schlesinger and M. C. Nussenzweig, *Nature*, 2015, **522**, 487-491.
116. S. A. Rosenberg and N. P. Restifo, *Science*, 2015, **348**, 62-68.
117. Y. B. Zhao, E. Moon, C. Carpenito, C. M. Paulos, X. J. Liu, A. L. Brennan, A. Chew, R. G. Carroll, J. Scholler, B. L. Levine, S. M. Albelda and C. H. June, *Cancer Research*, 2010, **70**, 9053-9061.
118. C. Rossig and M. K. Brenner, *Mol Ther*, 2004, **10**, 5-18.
119. M. Kalos and C. H. June, *Immunity*, 2013, **39**, 49-60.
120. A. Varela-Rohena, C. Carpenito, E. E. Perez, M. Richardson, R. V. Parry, M. Milone, J. Scholler, X. Hao, A. Mexas, R. G. Carroll, C. H. June and J. L. Riley, *Immunol Res*, 2008, **42**, 166-181.
121. L. Chang, D. Gallego-Perez, X. Zhao, P. Bertani, Z. Yang, C. L. Chiang, V. Malkoc, J. Shi, C. K. Sen, L. Odonnell, J. Yu, W. Lu and L. J. Lee, *Lab Chip*, 2015, **15**, 3147-3153.
122. A. Khvorova, A. Reynolds and S. D. Jayasena, *Cell*, 2003, **115**, 209-216.
123. B. Mansoori, S. Sandoghchian Shotorbani and B. Baradaran, *Adv Pharm Bull*, 2014, **4**, 313-321.
124. A. Fire, S. Xu, M. K. Montgomery, S. A. Kostas, S. E. Driver and C. C. Mello, *Nature*, 1998, **391**, 806-811.
125. J. Tabernero, G. I. Shapiro, P. M. LoRusso, A. Cervantes, G. K. Schwartz, G. J. Weiss, L. Paz-Ares, D. C. Cho, J. R. Infante, M. Alsina, M. M. Gounder, R. Falzone, J. Harrop, A. C. White, I. Toudjarska, D. Bumcrot, R. E. Meyers, G. Hinkle, N. Svrzikapa, R. M. Hutabarat, V. A. Clausen, J. Cehelsky, S. V. Nochur, C. Gamba-Vitalo, A. K. Vaishnaw, D. W. Sah, J. A. Gollob and H. A. Burris, 3rd, *Cancer Discov*, 2013, **3**, 406-417.
126. D. Gallego-Perez, J. J. Otero, C. Czeisler, J. Ma, C. Ortiz, P. Gygli, F. P. Catacutan, H. N. Gokozan, A. Cowgill, T. Sherwood, S. Ghatak, V. Malkoc, X. Zhao, W. C. Liao, S. Gnyawali, X. Wang, A. F. Adler, K. Leong, B. Wulff, T. A. Wilgus, C. Askwith, S. Khanna, C. Rink, C. K. Sen and L. J. Lee, *Nanomedicine*, 2016, **12**, 399-409.
127. K. Gao, X. Huang, C. L. Chiang, X. Wang, L. Chang, P. Boukany, G. Marcucci, R. Lee and L. J. Lee, *Mol Ther*, 2016, **24**, 956-964.
128. R. Maresch, S. Mueller, C. Veltkamp, R. Ollinger, M. Friedrich, I. Heid, K. Steiger, J. Weber, T. Engleitner, M. Barenboim, S. Klein, S. Louzada, R. Banerjee, A. Strong, T. Stauber, N. Gross, U. Geumann, S. Lange, M. Ringelhan, I. Varela, K. Unger, F. Yang, R. M. Schmid, G. S. Vassiliou, R. Braren, G. Schneider, M. Heikenwalder, A. Bradley, D. Saur and R. Rad, *Nat Commun*, 2016, **7**, 10770.
129. V. T. Chu, T. Weber, B. Wefers, W. Wurst, S. Sander, K. Rajewsky and R. Kuhn, *Nat Biotechnol*, 2015, **33**, 543-548.
130. K. Takahashi and S. Yamanaka, *Cell*, 2006, **126**, 663-676.
131. Saijilafu, E. M. Hur and F. Q. Zhou, *Nat Commun*, 2011, **2**, 543.
132. M. dal Maschio, D. Ghezzi, G. Bony, A. Alabastri, G. Deidda, M. Brondi, S. S. Sato, R. P. Zaccaria, E. Di

Fabrizio, G. M. Ratto and L. Cancedda, *Nat Commun*, 2012, **3**, 960.
133. J. L. Pinyon, S. F. Tadros, K. E. Froud, Y. W. AC, I. T. Tompson, E. N. Crawford, M. Ko, R. Morris, M. Klugmann and G. D. Housley, *Sci Transl Med*, 2014, **6**, 233ra254.
134. R. Phillips, *Physical biology of the cell*, Garland Science, New York, NY, Second edition / edn., 2013.
135. L. Chang, J. Hu, F. Chen, Z. Chen, J. Shi, Z. Yang, Y. Li and L. J. Lee, *Nanoscale*, 2016, **8**, 3181-3206.
136. C. Xie, Z. Lin, L. Hanson, Y. Cui and B. Cui, *Nat Nanotechnol*, 2012, **7**, 185-190.
137. L. Hanson, W. Zhao, H. Y. Lou, Z. C. Lin, S. W. Lee, P. Chowdary, Y. Cui and B. Cui, *Nat Nanotechnol*, 2015, **10**, 554-562.
138. F. Santoro, S. Dasgupta, J. Schnitker, T. Auth, E. Neumann, G. Panaitov, G. Gompper and A. Offenhausser, *ACS Nano*, 2014, **8**, 6713-6723.
139. K. Kitamura, B. Judkewitz, M. Kano, W. Denk and M. Hausser, *Nat Methods*, 2008, **5**, 61-67.
140. J. P. Giraldo-Vela, W. Kang, R. L. McNaughton, X. Zhang, B. M. Wile, A. Tsourkas, G. Bao and H. D. Espinosa, *Small*, 2015, **11**, 2386-2391.
141. A. K. Shalek, J. T. Gaublomme, L. Wang, N. Yosef, N. Chevrier, M. S. Andersen, J. T. Robinson, N. Pochet, D. Neuberg, R. S. Gertner, I. Amit, J. R. Brown, N. Hacohen, A. Regev, C. J. Wu and H. Park, *Nano Lett*, 2012, **12**, 6498-6504.
142. Y. H. Zhan, V. A. Martin, R. L. Geahlen and C. Lu, *Lab Chip*, 2010, **10**, 2046-2048.
143. S. Mahnic-Kalamiza, E. Vorobiev and D. Miklavcic, *J Membrane Biol*, 2014, **247**, 1279-1304.
144. G. Saulis, *Food Eng Rev*, 2010, **2**, 52-73.
145. T. Tryfona and M. T. Bustard, *Biotechnol Bioeng*, 2006, **93**, 413-423.
146. B. M. Chassy, A. Mercenier and J. Flickinger, *Trends Biotechnol*, 1988, **6**, 303-309.